J Therm Anal Calorim (2010) 99:423–429
DOI 10.1007/s10973-009-0408-6

Isothermal crystallization kinetics of fly ash filled *iso*-polypropylene composite- and a new physical approach

Dilip Chandra Deb Nath · Sri Bandyopadhyay · Aibing Yu · Darryl Blackburn · Chris White · Susy Varughese

Received: 2 February 2009 / Accepted: 30 July 2009 / Published online: 29 August 2009
© Akadémiai Kiadó, Budapest, Hungary 2009

Abstract Composites of pre-mixed fly ash (FA) and *isotactic*-polypropylene (PP) with varying degree of FA, 0, 20, 45 and 60 wt% were prepared by injection moulding at 483 K. The isothermal crystallization kinetics of the neat PP and composites are calculated using exotherms obtained from differential scanning calorimetry (DSC) at different isothermal crystallization temperatures (T_c) 403, 405 and 407 K. The lowest points of the exotherm peaks were shifted to higher crystallization times in the ranges of 0.75–1.50 min with the increasing of T_c in neat PP and composites regardless of FA percentage addition. The values of Avrami exponent n are found as non-integral number ranges $2 < n < 4$, and the calculated initial crystal thickness values of PP change slightly with increasing super cooling temperature as well as FA content.

Keywords Polypropylene · Fly ash · Composites · Isothermal crystallization · DSC

Introduction

PP based composites have a wide ranges of applications in many engineering and industrial atmosphere. At higher temperatures, semicrystalline polymers in polymer-filler composites show different thermal and mechanical properties. The degree of crystallinity and crystalline morphology depend on the type, size and shape of filler present in the polymer composite. The semicrystalline PP generally forms three different crystallographic phases, viz., α-monoclinic phase, *β*-pseudohexagonal phase and *γ*-orthorhombic phase. The pseudohexagonal *β*-crystalline phase melts at lower temperature, and more stable monoclinic α phase melts at higher temperature [1, 2].

The mechanical properties of PP can dramatically be improved by the addition of inorganic natural clay as reinforcement filler [3–8]. The selection of filler composed of PP is a critical task in designing and controlling the mechanical and thermal properties of composite. The mechanism of enhanced mechanical properties of PP composites is strongly related to the suppression, acceleration and/or formation of new crystalline structures of PP chains in the presence of filler. The filler in general influences the crystallization of α, *β* and *γ* forms and dimensional distribution of spherulites of PP in composites. The investigation of crystallization kinetics on filler nucleating function, therefore, will give direct evidence of alteration of crystalline phase of PP in composites. The crystallization kinetics can be studied under thermally stable and/or dynamic non-isothermal condition [9].

The potential nucleating fillers reported for crystallization of PP chains in PP-filler composites are glass fibre [10], calcium carbonate [11, 12], talc [13], carbon black [14], clay [15], kaolin [16], ZnO [17], carbon nanotube [18] and silica oxide [19, 20]. A number of studies have reported the utilization of industrial by-product FA as filler value added material in polymer composites, e.g., epoxy [21], polyester [22] and PP [23–26]. The tensile strength of the composite materials decreased with the addition of FA.

D. C. D. Nath · S. Bandyopadhyay (✉) · A. Yu
School of Material Science and Engineering, The University of New South Wales, Sydney, NSW 2052, Australia
e-mail: S.Bandyopadhyay@unsw.edu.au

D. Blackburn · C. White
Research and Ash Development, Cement Australia, Brisbane, QLD, Australia

S. Varughese
Department of Chemical Engineering, IIT Madras, Chennai 600 036, India

We recently reported that the composites of 20 wt% FA with PP showed 14% improvement in tensile strength at elevated test temperatures, 323 and 343 K with reduced brittle nature, which is now revision status elsewhere. In the case of non-isothermal behaviour analysed by DSC exotherms, the newly appeared peak was assigned to the crystallisation of β-phase in the presence of FA and the maximum 14% β-crystalline phase is formed with 45 wt% FA addition and the details of the nonisothermal crystallization kinetics were now reported separately [27]. On the other hand, FA is currently used in the formation of cement and concrete materials. Using FA in concrete is a well-known and established method and FA replaces up to 50% of cement without compromising concrete performance. This happens due to the pozzolanic and/or cementitious properties of FA [28]. In addition, the use of FA in concrete offers higher level benefits such as lower water requirements, improved workability, improved resistance to alkali aggregates, less heat hydration and less sulphur attack, as well as less permeability [29–31].

The objective of this work is to report the isothermal crystallization kinetics, which shows different phenomena from the non-isothermal conditions of PP in FA composites using Avrami equation and calculation of the initial crystal thickness using supercooling temperature.

Experimental procedure

Materials

The fly ash was obtained from Gladstone coal fire plant in Queensland, Australia. The ASTM D1505-03, 10 min melt flow index (MFI) of the PP is 60, indicating a low viscosity grade resin, which is suitable for preparation of composite samples in injection moulding.

Sample preparation

ASTM D 638 samples were prepared by injection moulding at 483 K from a pre-mix of white powdery PP with 20, 45 and 60 wt% FA in ball for three days.

Characterization

The thermal analysis was carried out using Perkin Elmer Differential Scanning Calorimeter (DSC) TAC-7/DX. About 5–7 mg samples were sealed in 30 μL aluminium pan with an empty aluminium pan used as reference, under nitrogen atmosphere. The rate of heating and cooling of the sample was 283, 288 and 293 K/min the range of −303 to 473 K, held for 2 min at 473 K to remove all the thermal history properly in non-isothermal condition. The second heating and cooling peaks were taken to evaluate the melting and crystallization temperature of the PP and composites. In the case of isothermal condition, the samples were quenched from 473 K with a rapid cooling rate of 473 K/min to a fixed isothermal temperature of crystallization (T_c) 403 and held for 10 min then cooled to 298 K by 283 K/min. The cycles were repeated to collect the crystallization exotherms at 405 and 407 K under an identical condition. The T_c has chosen in the middle of the melting (436 K) and glass transition temperatures (<373 K) of neat PP. The glass transition temperature was depended on the molecular weight and stereospecificity of PP and thermal condition, for example, *isotactic*-PP 373 K, *atactic*-PP −293 K and *syn*-PP −275 K [32, 33].

Results and discussion

Effect of isothermal crystallization temperatures on crystallization

The DSC exotherms at 403, 405 and 407 K of 20 wt% FA composite are shown in Fig. 1 as model. The mono-modal exotherms of α-crystal phase of PP chains were shifted to higher crystallization time by emerging broader peak with increasing T_c. At higher T_c, the translational mobility of PP chain in the crystal phase is slower due to the presence of higher level of free energy, representing the broaden peaks. A certain minimum temperature needs to overcome the kinetic barriers to complete a crystallization process. In the presence of spherical particles of FA, PP chains start nucleation to form a new crystalline β-phase and crystallize at lower temperature than the α-phase [34, 35].

The influence of FA on the crystallization process at 403 K is shown in Fig. 2. The crystallization peaks of composites shifted to higher crystallization time in the range of 0.75–1.2 min, although the onset crystallization times were almost identical. The slower crystallization rate in composites may occur due to getting the interruption of segmental motion of PP chains. The relationship of half time crystallization ($t_{½}$) with T_c is shown in Fig. 3. The $t_{½}$ in neat PP and composites increased with increasing T_c, and the slope of 45 wt% FA is double than that of the other composites. The equations of the lines were shown in Fig. 3.

The crystalline phenomena in neat PP, 20 and 60 wt% FA composites showed marginal differences in crystallization time and $t_{½}$ at any given T_c except in the case of 45% FA system. The case 45 wt% FA showed an unusual broaden peak and relatively higher $t_{½}$ values with increasing T_c.

A plausible explanation of the phenomena is offered by the authors considering the molecular structural

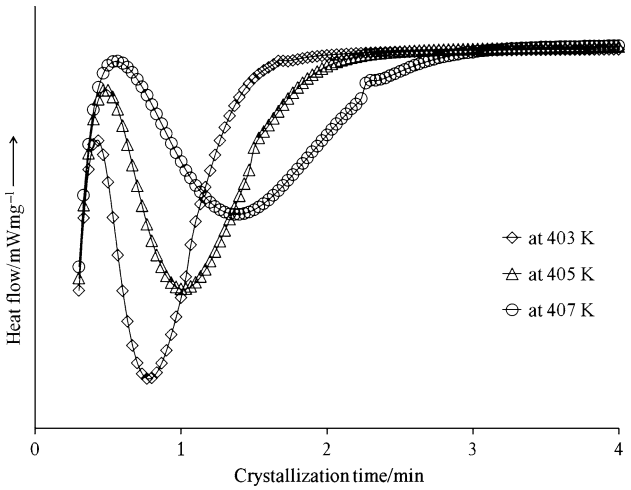

Fig. 1 DSC scans of isothermal crystallization of 20 wt% FA composite at different Temperatures/K

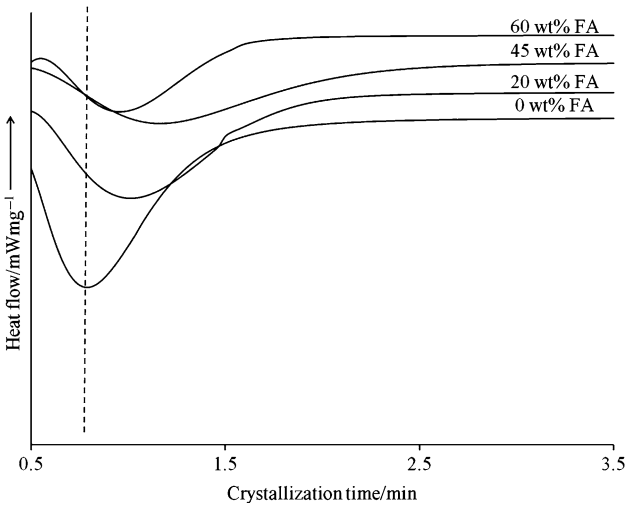

Fig. 2 DSC scans of crystallization of neat PP and composites at 403 K

arrangement of PP chains. The crystallization of the polymer comes from the aligned mobility of chain. In the case of composites, the polymer chains are linked to the surface of filler, and the level and strength of linking depends on the nature and concentration of the filler. There are three characteristic regions of the polymer chains in composite materials namely: immobilized, intermediate and mobile [36].

The parts of the polymer chain are immobilized on the surface of filler due to adherence of the two surfaces. Structural motions are restricted and have no role in crystallization. The intermediate region of the polymer is located slightly away from the surface of the filler particles, such that its dynamics are influenced by the strength of the filler and polymer interaction force. The mobile region is still further away from the filler particles hence motion is

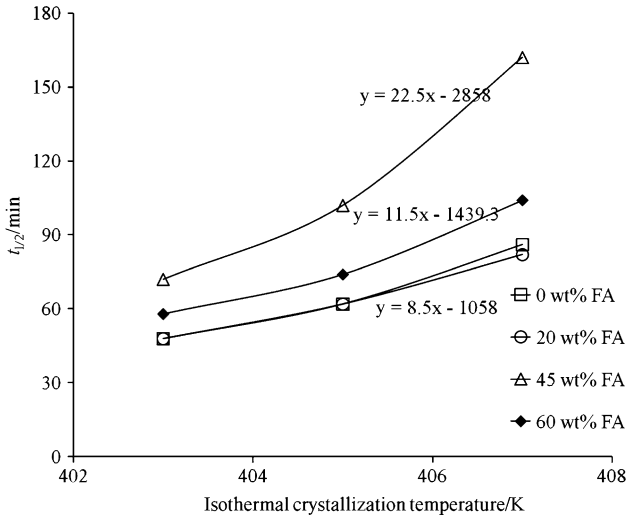

Fig. 3 Relationship of half time crystallization with isothermal crystallization temperatures in neat PP and composites

not restricted and it has a major role in crystallization [36, 37]. Several reports have contributed to the correlation of mechanical and thermal behaviours of composites with the morphological information provided schematic models by SEM images on FA and filler particles in polymer chains [36–38].

The segmental motion of PP chains in neat PP can diffuse smoothly from the melt state even in the less populated composite i.e. 20 wt% FA concentration. On the other hand, in the highly populated 60 wt% FA composite system, the crystallization of PP chains may occur in a localized manner at a given T_c due to entanglement of PP chains in interstitial voids between spherical filler particles. The inter-particle space arises from the agglomeration of the spherical particles [39]. In the case of 45 wt% FA, the diffusible PP chains may face strong interruption in the inter-layer of two particles. The crystallization, therefore, may occur in sharing of free and inter layer of FA particles. As a result, PP segments in 45 wt% FA system form a transitional crystalline phase, and reveal a broaden scan [40]. The present SEM images in Fig. 4 of neat PP and composites support the plausible interpretation of crystallization and the localized area marked in the photographs. Based on the SEM images and crystallization behaviour, we have developed a physical model, shown schematically in Fig. 5 to illustrate the position of FA particles and PP chains in 20, 45 and 60% FA systems [36–38].

Isothermal crystallization kinetics

The differential heat (dH/dt) evolved during rapid cooling from melt was recorded as a function of crystallization time at a given crystallization temperature. The relative crystallinity X_t of crystallized material can be calculated using

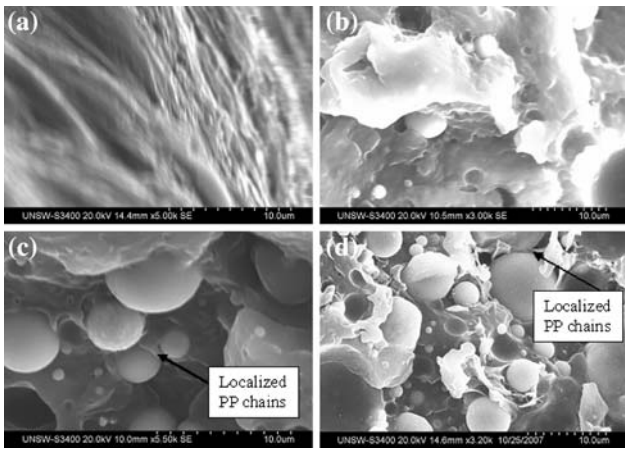

Fig. 4 SEM images of **a** neat PP. **b** 20 wt%. **c** 45 wt%. **d** 60 wt% FA composites

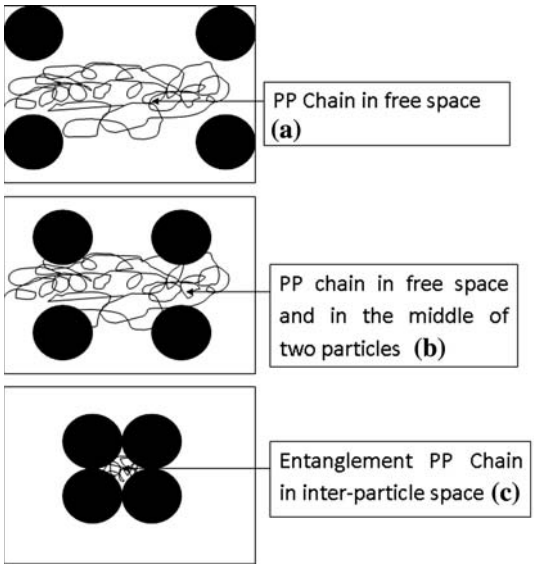

Fig. 5 A proposed physical scheme of polymer chain and FA particle interaction in **a** 20 wt%. **b** 45 wt%. **c** 60 wt% FA composites

the integral equation reported in references and using Fig. 1 [41, 42]. The Avrami equation is used to calculate the isothermal crystallization kinetics of neat PP and composites [43].

$$1 - X_t = \exp(-Z_t t^{\mathrm{n}}) \quad (1)$$

where, X_t is the relative degree of crystallinity for crystallization time t, Z_t is crystallization constant involving both the nucleation and growth rate of crystal and n is the Avrami exponent parameter related to the crystal dimension. There is a strong meaningful significance in isothermal steady condition between Avrami exponent n and crystallization constant Z_t [44]. The double-logarithmic of Eq. 1 was derived as Eq. 2 to plot the relationship of $\ln[-\ln(1 - X_t)]$ against $\ln t$ in Fig. 6.

$$\ln[-\ln(1 - X_t)] = \ln Z_t + n \ln t \quad (2)$$

The integrated DSC exotherms of neat PP and composites give straight lines and fit well with the Avrami model at different T_c. The values of n and Z_t were calculated from the slope and the intercept of the yielding straight line curves, respectively.

The n values of PP and composites in the ranges of 2–4 were unaffected by the addition of FA and different T_c. However, the Z_t values decreased slightly with respect to T_c. The values of n and Z_t in general are influenced by the nature of nucleation and molecular weight of polymer as well as the thermal condition. In non-isothermal condition, n values of composites show values <2 than isothermal condition. The Avrami exponent n values of composite systems are similar to those of in glass fibre/PP composites [42] and higher values (2.7 ~ 5) were observed in kenaf fibre-PP system [44]. Higher n values reflect the existence of a specific number of three-dimensional spherulite growths in PP and composites [12, 44]. The relationship of n as a function of T_c in composites is shown in Fig. 7. The slope of curve decreases in PP while it shows slight increase and then decrease in the case of composites.

Effect of FA on crystallization temperature in composites

FA in composite was identified as β-nucleating agent due to the formation of β-crystalline phase of PP chains. The intensity of β-crystalline phase was increasing with increasing concentration of FA in composite, and the maximum degree of β-crystallinity were calculated as 14% with 45 wt% FA addition [27]. The crystallization

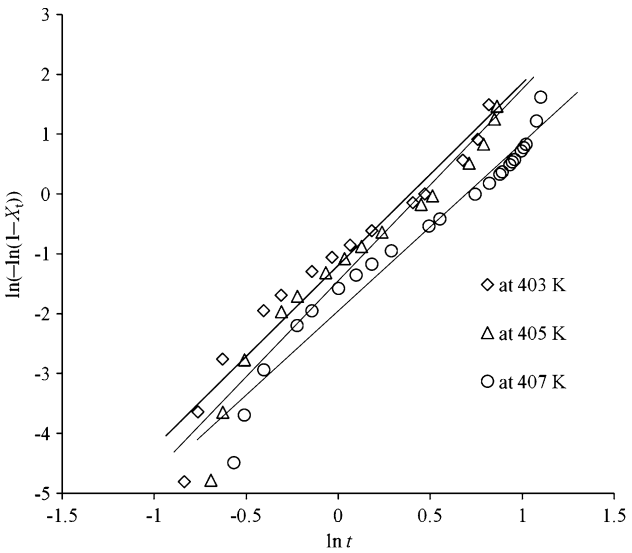

Fig. 6 Avrami plot of isothermal crystallization for 20 wt% FA composite

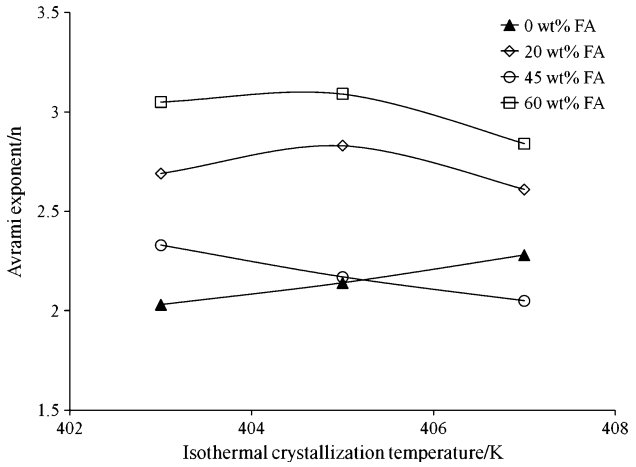

Fig. 7 Relationship of Avrami exponent with crystallization temperatures of neat PP and composites

temperature (T_{cry}), melting temperature (T_m) and supercooling temperature (ΔT) of the PP and composites are shown in Table 1.

The effect of FA content on non-isothermal crystallization temperature is shown in Fig. 8 with cooling rates, 283, 288 and 293 K/min. Fig. 8 shows that the cooling rates have significant level of influence on the crystallization temperatures. A slight increase in crystallization temperature in 20 wt% FA system results in an early crystallization due to the possible enhanced crystallization effect of FA. The accelerated nucleation effect of 20 wt% FA helps to convert some part of amorphous chains to crystalline chains, and initiates the formation of a new β-crystalline phase. On increasing the FA content, the β-phase increases and the α-phase decreases (the β-phase is not shown in Fig. 8).

Table 1 Non-isothermal crystallization and melting temperatures of α-phase in polypropylene and composites at different cooling rates

FA/%	Cooling rate/K	T_{cry}/K	T_m/K	$\Delta T = (T_m - T_{cry})$/K
0	283	399.3	438	38.7
	288	396	437.6	40.6
	293	394.3	436.1	42.8
20	283	400.3	439.4	39.1
	288	398	436.6	38.6
	293	395.6	436.4	40.8
45	283	396.6	436.4	39.7
	288	395.1	435.1	40.1
	293	393	435.1	42.1
60	283	396.3	441.4	43.1
	288	394.5	435.6	41.1
	293	392.3	435.7	43.5

Calculation of initial crystal thickness

Crystallization of polymer primarily is reflecting the generation and growth of lamella in solution and/or in melt state. The thickness of lamella essentially implies to the corresponding fold length. Equation 3 provides a relationship between initial lamella thickness and the supercooling temperature [45].

$$L_c* = 276.4/\Delta T + 4.16 \quad (3)$$

where L_c*, initial crystal thickness in nm and ΔT, supercooling temperature. They conclude that the initial crystal thickness is inversely proportional to the supercooling temperature and this dependence has led to the development of the kinetic theories of chain folding. The kinetic theory permits to predict and calculate the initial thickness of crystal and growth rates quantitatively.

We, therefore, have taken attempts to calculate the initial crystal thickness of PP using Eq. 3 of neat PP and composite systems from melt states. The values of L_c* are plotted as a function of ΔT in Fig. 9.

All the data points L_c* in fact are in one line and show inversely proportional to ΔT. A similar trend was reported in the original research paper in the case of crystallization of polyethylene [45]. The initial crystal thickness of PP do not get influenced significantly in the presence of spherical particles FA and different concentrations, although it is apparently believed that the growth of crystal will face some interruption due to the presence of varying size spherical particles FA as immobilized solid phase in the systems as shown in SEM images in Fig. 4. In the absence of FA, the lamella appears unidirectional-rodlike structure initially, and then develops as bundle growth along with branching, fanning twisting, and finally forms spherulites by diffusion of molecular segments [46]. In the presence of

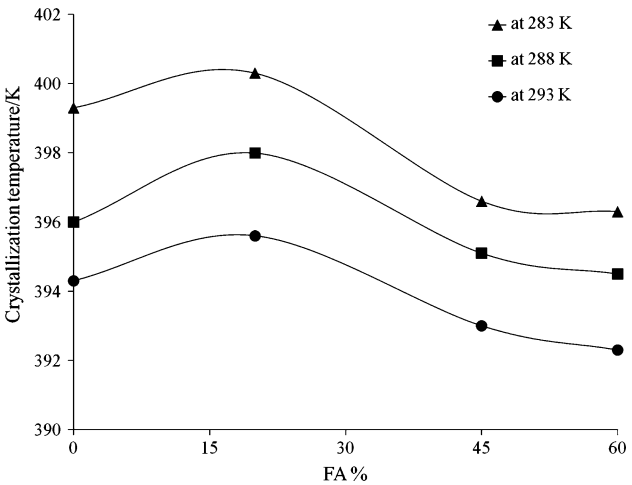

Fig. 8 The effect of FA on the non-isothermal crystallization temperature with different cooling rates/min

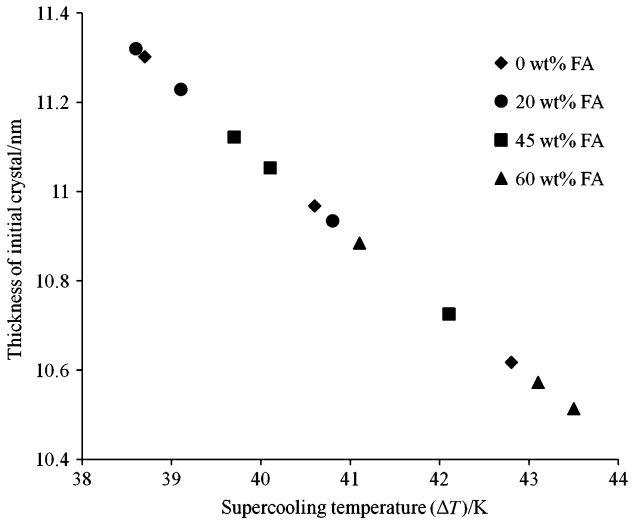

Fig. 9 The relationship of initial thickness of crystal with supercooling temperatures in neat PP and composites

FA particles, the diffusible molecular segments face hindrance effect as a result the trend of unidirectional lamella growth turns to multidirectional and occurs in scattered fashion. The scattered behaviour of lamella growth is more severe in the highly populated 60 wt% FA system, and completely turns in only localized crystallization in the entangled area around the FA particles as shown in schematic diagram Fig. 5.

Conclusions

The isothermal crystallization kinetics of neat PP and composites were studied using DSC exotherms and the results are summarized below:

1. The shifting of mono-modal crystallization exotherms to higher crystallization time regardless of PP and FA percentage to composites indicated that crystallization became slower with increasing T_c. The half crystallization time ($t_{½}$) of PP and composites were also increased proportionally with increasing T_c, although the onset crystallization time was almost independent.
2. The crystalline phenomena did not show any big differences in PP, 20 and 60 wt% composites except 45 wt% FA composite. The composite 45 wt% FA showed relatively higher $t_{½}$ values with increasing T_c. The plausible explanation is that the molecular segmental motion of PP chain suffers less steric hindrance in the less concentrated 20 wt% FA, and in the 60 wt% case, only localized crystallization occurs. In the case of 45 wt% FA system, the dual crystallization phenomena in localized and diffusible motion between the inter-particles distance are prominent. As a result, it takes longer time and forms a transitional crystalline phase with broaden peak.
3. The values of Avrami exponent n were found as non-integral number $2 < n < 4$ and verified the existence of a specific number of three-dimensional crystalline growth in PP and composites irrespective of FA concentration.

Finally, the initial crystal thickness was calculated using supercooling relationship equation, and the values are almost identical irrespective of FA added to the systems. The calculated values have a good agreement with reported values elsewhere.

Acknowledgements Dilip Chandra Deb Nath is grateful to ARC (Australian Research Council) for full financial support in the linkage program study (Project: ARC LP0669837).

References

1. Li JX, Cheung WL. A correction function to determine the β-fusion heat in a mixture of α and β-PP. J Therm Anal Calorim. 2000;61:757–62.
2. Lotz B, Wittmann JC, Lovinger JA. Structure and morphology of poly(propylenes): a molecular analysis. Polymer. 1996;37(22):4979–92.
3. Giammelis EP. Polymer layered silicate nanocomposites. Adv Mater. 1996;8(1):29–35.
4. Messersmith PB, Giannelis EP. Synthesis and barrier properties of poly(ecapro1actone)-layered silicate nanocomposites. J Polym Sci Part A: Polym Chem. 1995;33:1047–57.
5. Okamoto M, Nam PH, Maiti P, Kotaka T, Hasegawa N, Usuki A. A house of cards structure in polypropylene/clay nanocomposites under elongation flow. Nano Lett. 2001;1(6):295–8.
6. Usuki A, Kawasumi T, Fukushima Y, Okada A. Mechanical properties of nylon 6-clay hybrid. J Mater Res. 1993;8:1179–82.
7. Srinivas S, Basu JR, Riffle JS, Wilkes GL. Kinetics of isothermal and nonisothermal crystallization of novel poly(ary1ene ether ether sulfide)s. Polym Eng Sci. 1997;37(3):497–510.
8. Xie XL, Li RKY, Tjong SC, Mai YW. Structural properties and mechanical behaviour of injection molded composites of polypropylene and sisal fiber. Polym Compos. 2002;23(3):319–328.
9. Acosta JL, Ojeda MC, Morales E, Linares A. Morphological, structural, and interfacial changes produced in composites on the basis of polypropylene and surface-treated sepiolite with organic acids. 111. isothermal and nonisothermal crystallization. J Appl Polym Sci. 1986;32:4119–26.
10. Gaceva GB, Janevsky A, Mader E. Nucleation activity of glass fibers toward *i*PP evaluated by DSC and polarizing light microscopy. Polymer. 2001;42:4409–16.
11. Zhang QX, Yu ZZ, Xie XL, Mai YW. Crystallization and impact energy of polypropylene/$CaCO_3$ nanocomposites with non-ionic modifier. Polymer. 2004;45:5985–94.
12. Jancar J, Kucera J. Yield behavior of PP/$CaCO_3$ and PP/$Mg(OH)_2$ composites. II: enhanced interfacial adhesion. Polym Eng Sci. 1990;30:714–20.
13. Ferrage E, Martin F, Boudet A, Petit S, Fourty G, Jouffet F, et al. Talc nucleating agent in polypropylene: morphology induced by lamellar particles addition and interface miner-matrix modelization. J Mater Sci. 2002;37:1561–73.
14. Chen J, Li X, Wu C. Crystallization behaviour of polypropylene filled with modified carbon black. Polym J. 2007;39(7):722–30.

15. Kim B, Lee SH, Lee D, Ha B, Park J, Char K. Crystallization kinetics maleated polypropylene/clay hybrids. Ind Eng Chem Res. 2004;43:6082–9.
16. Mucha M, Krolikowski Z. Application of DSC to study characterization kinetics of polypropylene containing fillers. J Therm Anal Calorim. 2003;74:549–57.
17. Tang JG, Wang Y, Liu YH, Belfiore LA. Effects of organic nucleating agents and zinc oxide nanoparticles on isotactic polypropylene crystallization. Polymer. 2004;45:2081–91.
18. Valentini L, Biagiotti J, Kenny JM, Santucci S. Effects of single-walled carbon nanotubes on the crystallization behaviour of polypropylene. J Appl Polym Sci. 2003;87:708–13.
19. Papageorgiou GZ, Achilias DS, Bikiaris DN, Karayanndis GP. Crystallization kinetics and nucleation activity of filler in polypropylene/surface-treated SiO_2 nanocomposites. Thermochim Acta. 2005;427:117–128.
20. Rong MZ, Zhang MQ, Pan SL, Lehmann B, Friedrich K. Analysis of the interfacial interactions in polypropylene/silica nanocomposites. Polym Int. 2004;53:176–83.
21. Gupta N, Brar BS, Woldesenbet E. Effects of filler addition on the compressive and impact properties of glass fibre reinforced epoxy. Bull Mater Sci. 2001;24(2):219–23.
22. Guhanathan S, Sarojadevi M. Studies on interface in polystyrene/fly ash particulate composites. Compos Interface. 2000;11(1):43–66.
23. Wong KWY, Truss RW. Effect of fly ash content and coupling agent on the mechanical properties of fly ash-filled polypropylene. Compos Sci Technol. 1994;52:361–8.
24. Wang M, Shen Z, Cai C, Ma S, Xing Y. Experimental investigations of polypropylene and polyvinyl chloride composites filled with plerospheres. J Appl Polym Sci. 2004;92:126–31.
25. Jarvela PA, Jarvela PK. Multicomponent compounding of polypropylene. J Mater Sci. 1996;31:3853–60.
26. Huang X, Hwang JY, Gillis JM. Processed low NO_x fly ash as filler in plastics. J Min Mater Charact Eng. 2003;2(1):11–31.
27. Nath DCD, Bandyopadhyay S, Yu A, Blackburn D, White C. Novel observations on kinetics of non-isothermal crystallization in fly ash filled isotactic-polypropylene composites. J Appl Polym Sci. 2009; in press.
28. Sun P, Wu CH. Transition from brittle to ductile behavior of fly ash using PVA fibers. Cem Concr Compos. 2008;30:29–36.
29. Hidalgo A, García JL, Alonso MC, Fernández L, Andrade C. Microstructure development in mixes of calcium aluminate cement with fume or fly ash. J Therm Anal Calorim. 2009;96(2):335–45.
30. Komljenovi M, Stojkanovi LP, Baarevi Z, Jovanovi N, Rosi A. Fly ash as the potential raw mixture component for Portland cement clinker synthesis. J Therm Anal Calorim. 2009;96(2):363–8.
31. Rahhal V, Talero R. Fast physics-chemical characterization of fly ash. J Therm Anal Calorim. 2009;96(2):369–74.
32. Stevens MP. Polymer chemistry: an introduction. 3rd ed. New York: Oxford University Press; 1999.
33. http://faculty.uscupstate.edu/llever/Polymer%20Resources/GlassTrans.htm. Accessed 1st July, 2009.
34. Organ SJ, Ungar G, Keller A, Wills HH. Isothermal refolding in crystals of long alkanes in solution. 11. morphological changes accompanying thickening. J Polym Sci Part B: Polym Phys. 1990;28:2365–84.
35. Barham PJ, Chivers RA, Keller A, Martinez-Salazar J. The supercooling dependence of the initial fold length of polyethylene crystallized from the melt: unification of melt and solution crystallization. J Mater Sci. 1985;20:1625–30.
36. Litvinov VM, Steeman PAM. EPDM-carbon black interactions and the reinforcement mechanisms, as studied by low-resolution ^{1}H NMR. Macromolecules. 1999;32:8476–90.
37. Sridhar V, Xiu ZZ, Xu D, Lee SH, Kim JK, Kang DJ, et al. Fly ash reinforced thermoplastic vulcanizates obtained from waste tire powder. Waste Manag. 2009;29:1058–68.
38. Lee SH, Balasubramanian M, Kim JK. Dynamic reaction inside co-Rotating twin screw extruder. II. Waste ground rubber tire powder/polypropylene blends. J Appl Polym Sci. 2007;106:3209–19.
39. Tan LS, Mchugh AJ. The role of particle size and polymer molecular weight in the formation and properties of an organoceramic composite. J Mater Sci. 1996;31:3701–6.
40. Lorenzo AT, Arnal ML, Mueller AJ, Boschetti-de-Fierro A, Abetz V. Nucleation and isothermal crystallization of the polyethylene block within diblock copolymers containing polystyrene and poly(ethylene-*alt*-propylene). Macromolecules. 2007;40(14):5023–37.
41. Xu W, Zhai H, Guo H, Whitely N, Pan WP. PE/ORG-MMT nanocomposites non-isothermal crystallization kinetics. J Therm Anal Calorim. 2004;78:102–12
42. Aella M, Martuscelli E, Sellitti C, Garagnani E. Crystallization behaviour and mechanical properties of polypropylene-based composites. J Mater Sci. 1987;22:3185–93.
43. Avrami MJ. Kinetics of Phase Change. III. Granulation, phase change, and microstructure. Chem Phys. 1941;9:177–84.
44. Grozdanov A, Burzarovska A, Bogoeva-Gaceva G, Avella M, Errico ME, Gentile G. Nonisothermal crystallization kinetics of kenaf fiber/polypropylene composites. Polym Eng Sci. 2007;5:745–9.
45. KTH Fibre and Polymer Technol "Morphology of semicrystalline polymers" Chapter 6, P186. http://www.polymer.kth.se/forskarutbildning/doktorandkurser/Chapter%206-1.pdf http://www.polymer.kth.se/forskarutbildning/doktorandkurser/Chapter%206-3.pdf, Accessed 1 July 2009.
46. Tjong SC, Li RK, Cheung T. Mechanical behavior of $CaCO_3$ particulate-filled beta-crystalline phase polypropylene composites. Polym Eng Sci. 2007;37(1):166–72.